Mechanisms of E × B Drift Rotation of a Vortex String in a Pure Electron Plasma*)

Yukihiro SOGA, Tetsuya MIMURA, Yasutada KATO and Youngsoo PARK

Kanazawa University, Kanazawa 920-1192, Japan

(Received 7 December 2012 / Accepted 20 February 2013)

Energy distribution of a pure electron plasma column rotating around the axis of a cylindrical vessel due to an $\boldsymbol{E} \times \boldsymbol{B}$ flow in a Malmberg–Penning trap is investigated. An abrupt relaxation of the energy distribution was observed in an electron string trapped for a few microseconds after injection from an electron emitter. The macroscopic $\boldsymbol{E} \times \boldsymbol{B}$ drift rotation of the electron column is mainly dominated by the microscopic axial energy distribution which determines the effective position of reflection at the end of the trap, that is, a radial electric field acting on the particles from an external trap potential.

Keywords: non-neutral plasma, 2D Euler fluid, vortex filament, $\boldsymbol{E} \times \boldsymbol{B}$ drift rotation, parallel energy analysis

DOI: 10.1585/pfr.8.2401034

1. Introduction

Many features of the dynamics of Euler fluids have been experimentally examined using electron plasmas confined in a Malmberg–Penning trap [1–5]. The two-dimensional macroscopic dynamics of an electron plasma in a plane transverse to a strong homogeneous magnetic field, trapped axially by an electrostatic potential, are isomorphic to that of an inviscid, incompressible Euler fluid, as long as the axial bouncing motion of the electrons is significantly faster than the transverse $\boldsymbol{E} \times \boldsymbol{B}$ drift motion of their guiding centers. The string-shaped distribution of electrons acts as a vortex string [3–5]. To understand the motion of a vortex string or a vortex filament is fundamental to the study of fluid dynamics.

An electron string injected off axis in a cylindrical trap is expected to rotate around the axis of the cylindrical vessel due to $\boldsymbol{E} \times \boldsymbol{B}$ drift, maintaining its string structure as long as the rotation is much slower than the rotation of the string on its axes [6–8]. The electric field driving the $\boldsymbol{E} \times \boldsymbol{B}$ drift consists of a self-field from its image charge and an external field from the vacuum potential. In early study, the effect of the two electric fields was experimentally observed, however, for the theoretical estimation of the observed rotation frequency, it was assumed that the energy of electrons in the string remained constant and equal to the injection energy of the initial electron beam [8, 9]. In this study, we focused on the macroscopic $\boldsymbol{E} \times \boldsymbol{B}$ rotation frequency of an electron string around the vessel axis by concentrating on the microscopic dynamics of the electrons. The rotation frequency was estimated by an experiment and a theoretical calculation based on the measured energy distribution functions of the electron string.

author's e-mail: ysoga@staff.kanazawa-u.ac.jp

*) This article is based on the presentation at the 22nd International Toki Conference (ITC22).

2. Theoretical Background

The configuration studied here consisted of an electron string with an effective infinite length running axially in a cylindrical vessel immersed in a strong magnetic field $\boldsymbol{B} = B\hat{z}$ and with a radial distance r from the central axis. The radial extent of the electrons in the transverse plane was much smaller than the radius of the cylindrical conductive wall; thus, the electron string is assumed to be an infinitely long line charge. The rotation frequency Ω of the electron string under a radial electric field E_r is represented as $\Omega = E_r/rB$. In the experiment, the frequency Ω is considered as the sum of the frequency Ω^{self} driven by an electric field E^{self} from an image charge and the frequency Ω^{ext} driven by the electric field E^{ext} of a trap potential acting at the plasma ends [9].

2.1 Image charge effect

The dynamics of an infinitely long line charge can be described as an equation of motion in mechanics. A line charge with a charge density $-\lambda$ at a position $\boldsymbol{r_0} = r_0\hat{r}$ induces an image charge on the cylindrical conductive wall with a radius R to preserve an equipotential surface. The electric field in the cylinder from the induced charge on the wall is equal to that from an image line charge at a position $r_1 = (R^2/r_0)\hat{r}$ with a line density λ. The electric potential at a position r created by the two line charges is

$$\phi(r) = -\frac{\lambda}{2\pi\varepsilon_0}\left(\ln|r - r_0| - \ln|r - r_1|\right) + C. \tag{1}$$

To satisfy the experimental condition $\phi(R) = 0$, the constant is given by

$$C = \frac{\lambda}{2\pi\varepsilon_0}\ln\frac{r_0}{R}. \tag{2}$$

Therefore, the potential created by the image line charge is represented as

$$\phi^{self}(r) = \frac{\lambda}{2\pi\varepsilon_0}\left\{\ln(r_1 - r) + \ln\frac{r_0}{R}\right\}, \tag{3}$$

and the electric field acting on the string is

$$E_r^{self}(r_0) = -\left.\frac{\partial\phi^{self}(r)}{\partial r}\right|_{r=r_0} = \frac{\lambda}{2\pi\varepsilon_0}\frac{r_0}{r_0^2 - R^2}. \tag{4}$$

The rotation frequency driven by the image charge is

$$\Omega^{self}(r_0) = -\frac{E_r^{self}(r_0)}{r_0 B} = \frac{\lambda}{2\pi\varepsilon_0 B}\frac{1}{R^2 - r_0^2}. \tag{5}$$

As a result, the rotation frequency of an electron string with a length L and an electron number N at a position r_0 driven by a self-electric field can be obtained by

$$\Omega^{self} = \frac{eN}{2\pi\varepsilon_0 BL\left(R^2 - r_0^2\right)}. \tag{6}$$

2.2 External field effect

We can estimate the rotation frequency Ω^{ext} driven by the external radial electric field E_r^{ext} from a trap potential even if an electron plasma does not exist. A negative voltage applied to two cylindrical electrodes at the ends of the trap produces an approximate harmonic electric potential as a function of the radius around the trap ends. The effective electric field acting on the electrons traveling from the center of the trap $z = 0$ to the reflection position $z = z_t$ is given by

$$\langle E_r^{ext}\rangle = \frac{\int_0^{z_t} E_r^{ext}(z)\cdot v_z^{-1}(z)\mathrm{d}z}{\int_0^{z_t} v_z^{-1}(z)\mathrm{d}z}. \tag{7}$$

Since we can assume that the potential of electrons is much smaller than their kinetic energy, the axial electron velocity is expressed as

$$v_z(z) = \sqrt{\frac{2\left(E + e\phi^{ext}(z)\right)}{m}}. \tag{8}$$

The reflection position z_t is a function of the parallel energy E, because $v_z(z)$ depends on E. If we average over particles based on the energy distribution function $f(E)$, the ensemble average of $\langle E_r^{ext}\rangle$ can be expressed as

$$\overline{\langle E_r^{ext}\rangle} = \int_0^{\infty}\langle E_r^{ext}\rangle\cdot f(E)\,\mathrm{d}E, \tag{9}$$

where the distribution function $f(E)$ can be determined by an experiment. Thus, the rotation frequency Ω^{ext} is given by

$$\Omega^{ext} = \frac{\overline{\langle E_r^{ext}\rangle}}{r_0 B}. \tag{10}$$

3. Experimental Method

The electron plasma is confined in the Malmberg–Penning trap that combines a radial constraint with a homogeneous magnetic field of $B = 0.1$ T and axial reflections between -80 V potential dips at both ends. As shown in Fig. 1, the potential is created by negatively biasing the end cylindrical electrodes and 9 axially aligned cylindrical electrodes. Of the 11 electrodes, which are numbered from 1 to 11 from the cathode side, the 3rd, 6th, 9th electrodes are azimuthally divided into four sectors with a uniform separation of $\pi/2$. An electron string is generated by injecting electrons from the thermionic cathode on the left side.

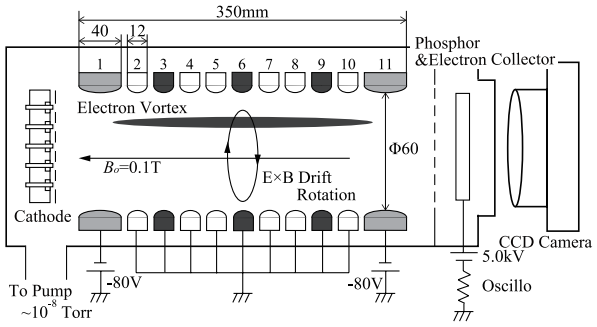

Fig. 1 Schematic configuration of a vortex filament experiment with a pure electron plasma.

For rotation frequency measurements, we detect the time evolution of the image current of the electron string. The FFT analysis of the signal shows the rotation frequency of the electron string. We connect one of 6th sector electrodes to the virtual ground of a current amplifier by a resistance of 15 kΩ. Unbalanced grounding or even careless connection of a high-gain amplifier can cause unstable oscillations of the electron column due to diocotron instability [10]. Hence we carefully adjust the resistance of this sector while all other electrodes are directly grounded to the vacuum chamber wall.

The method of analyzing the axial kinetic energy of electrons is as follows [11]. After the electron plasma is confined for an arbitrary time, the electrons are dumped by a lowered, but non-zero, confinement potential. Electrons with sufficient energy escape from the potential barrier along the magnetic field lines and are collected at a phosphor screen that is placed at the end of the trap on the right side in Fig. 1. We measured both the total electron number and the luminosity distribution of phosphor. By repeating the procedure with various barrier potentials, we measured a number of electrons Q_{esc} as a function of the energy E. By differentiating the data, we obtained the parallel energy distribution of the electrons

$$f(E) = -\frac{\mathrm{d}}{\mathrm{d}E}\frac{Q_{esc}(E)}{Q_{all}}. \tag{11}$$

4. Experimental Observation and Analysis

4.1 Measurement of rotation frequency

Figure 2 shows the rotation frequency and the radius of the electron string as a function of the holding time t for

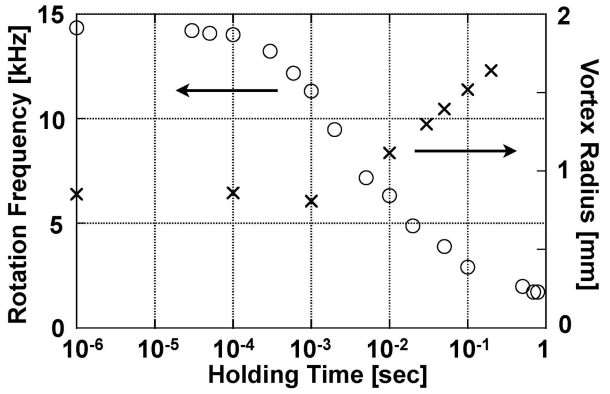

Fig. 2 Rotation frequency (open circle) and vortex radius in a transverse profile of an electron string (cross) are plotted as a function of holding time. Vortex radius is defined as a half-width at half-maximum in the density profile of an electron string on the cross section.

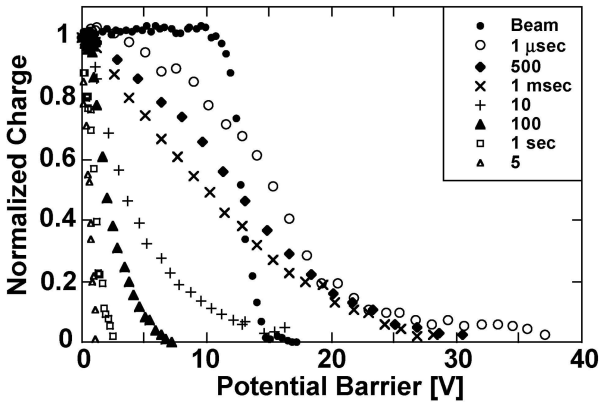

Fig. 3 Normalized electron numbers escaping from a potential barrier applied to the end of the trap for different holding times. All electrons can escape at potential 0 V.

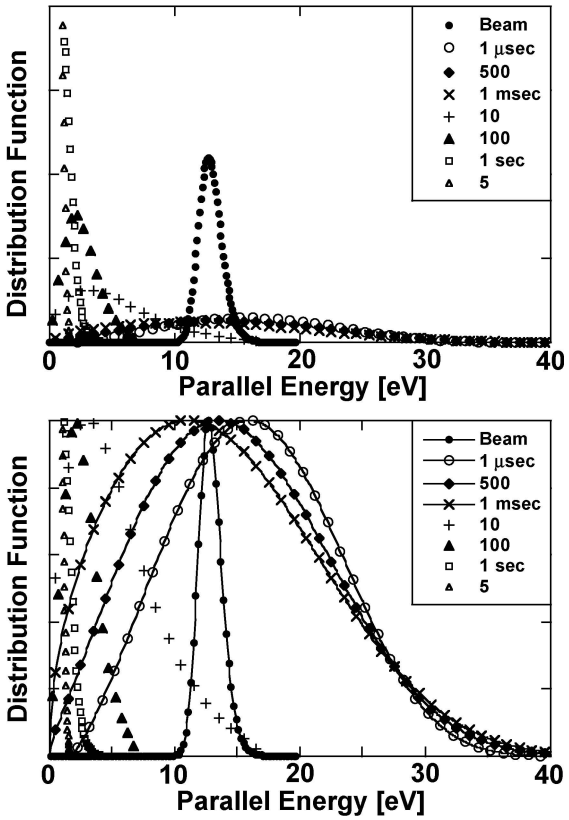

Fig. 4 Energy distribution function of the electron string calculated from the data in Fig. 3. Initial electron beam accelerated at A-K voltage of 15 V. The lower figure represents profiles normalized by each maximum value in the ordinate to distinguish closely resembling distributions.

which the electron plasma is confined. An electron string with 6×10^6 electrons, an axial length of 0.17 m, and a radius of 0.8 mm is injected at a radial position of 15 mm. It rotates with a constant frequency of 14.5 kHz for several rotations. After $t = 100\,\mu$s, the rotation frequency decreases, and finally only 12% of the initial frequency was observed at $t = 1$ s. The vortex radius is constant for 1 ms and after that time period, it linearly increases because of radial dissipation.

4.2 Measurement of parallel energy distribution

Figure 3 shows observed number of electrons, that escaped from a potential barrier as a function of the barrier height. Initial electrons injected as a beam with an acceleration voltage of 15 V show a rapid decrease at a barrier potential of around 15 V as indicated by the closed circles. Until a holding time of $t = 1$ ms, there is a moderate decrease in the electron number in the wide range of the barrier potential from 0 V to over 30 V. All electrons are trapped at a barrier of less than 7 V after $t = 100$ ms.

According to Eq. (11), the parallel energy distribution of the electron string was calculated as a function of the holding time, as shown in Fig. 4. The energy distribution shows a loosely expanded distribution from low energy to a high energy of 36 eV at a holding time of $t = 1\,\mu$s during which the electrons reflect three or four times between −80 V potential dips at both ends and mostly do not rotate. The peak energy of the electron string gradually decreases for a holding time from $t = 1\,\mu$s to 1 ms. After that time period, a rapid decrease was observed, and the relaxation state was realized after 100 ms. The average energy of the electron string slowly decreases over 1 s as shown in Fig. 5.

4.3 Estimation of rotation frequency

We shall determine the rotation frequency theoretically. The ensemble of the effective external electric field $\langle E_r^{ext} \rangle$ given by Eq. (9) was calculated as a function of time. Here the energy distribution function $f(E)$ in Fig. 4 was used. The calculated rotation frequencies are plotted in Fig. 6. The measured frequencies (open circles) are in good agreement with the calculated frequencies (open squares) contributed by a bounce-averaged external electric field. The macroscopic $\boldsymbol{E}\times\boldsymbol{B}$ drift rotation of the single

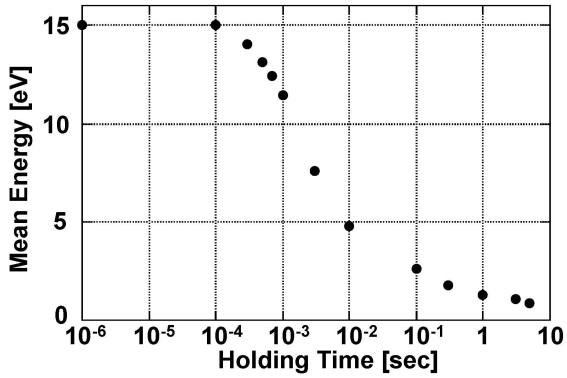

Fig. 5 Mean energy of the electron string calculated by eq (9) as a function of holding time.

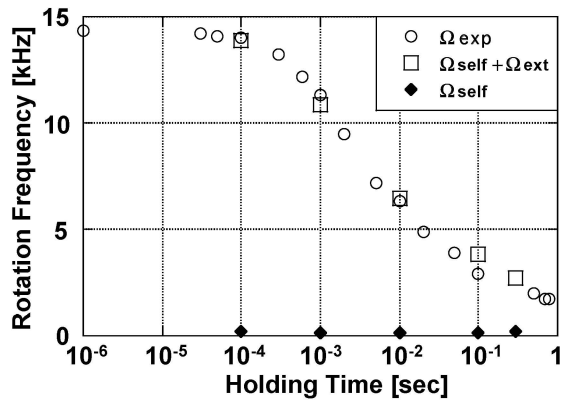

Fig. 6 Rotation frequencies of the electron string are plotted as a function of holding time with open circles (experiment) and open square (theory). Rotation caused by the self-field (indicated by closed squares) represents only 2% of the rotation caused by the external field.

electron column is mainly dominated by the microscopic energy distribution which determines the effective position of the reflection; that is, a radial electric field attributed to an external trap potential exerted on the particles.

5. Discussion and Conclusion

In this experiment, the rotation frequency of the electron string is mainly determined by the external field. For a study of Euler fluids using electron plasmas in the Malmberg–Penning trap, to assure axial homogeneity, more dense plasmas in a longer confinement region are generally adopted [1–5]. However, even in these plasmas, the external effect on the rotation frequency may not be negligible. If the effect of the $\boldsymbol{E} \times \boldsymbol{B}$ rotation of electrons driven by the external field is independent of their radial position, we can identify the 2D motion of the plasma with that of an isolated Euler fluid. However, in the experiment using an initial distribution of electrons prepared from the thermally relaxed electrons and a beam with an energy peak [3–5], the external effects are different between them. As a result, a velocity shear from the external field always exists, and we cannot consider the situation as an isolated system.

Relaxation of the energy distribution function can be explained in three steps. First, an abrupt expansion of the energy distribution was observed right after the confinement. We speculate that the phenomenon arises from the two-stream instability of the bouncing electrons or the axial acceleration of some electrons due to switching the trap potential at electron injection. Next, relaxation occurs after an order of milliseconds because of the Coulomb collision. We suppose that the axial kinetic energy of electrons is converted into perpendicular energy, and then the Maxwell distribution is realized at $t = 100$ ms. Finally, neutral collision causes relaxation after several hundred milliseconds at a background pressure of 10^{-8} Torr. As a result, the electron temperature decreases to less than 1 eV at a holding time of $t = 5$ s.

In summary, we investigated the $\boldsymbol{E} \times \boldsymbol{B}$ rotation mechanism using a single electron column, and we measured their parallel energy distribution. The macroscopic $\boldsymbol{E} \times \boldsymbol{B}$ drift rotation of the single electron column is mainly dominated by the microscopic energy distribution which determines the effective position of the reflection, that is, a radial electric field attributed to an external trap potential exerted on the particle.

[1] C.F. Driscoll and K.S. Fine, Phys. Fluids B **2**, 1359 (1990).
[2] K.S. Fine, A.C. Cass, W.G. Flynn and C.F. Driscoll, Phys. Rev. Lett. **75**, 3277 (1995).
[3] Y. Kiwamoto, K. Ito, A. Sanpei and A. Mohri, Phys. Rev. Lett. **85**, 3173 (2000).
[4] Y. Soga, Y. Kiwamoto, A. Sanpei and J. Aoki, Phys. Plasmas **10**, 3922 (2003).
[5] A. Sanpei, Y. Kiwamoto, K. Ito and Y. Soga, Phys. Rev. E **68**, 016404 (2003).
[6] S.A. Prasad and T.M. O'Neil, Phys. Fluids **22**, 278 (1979).
[7] A.J. Peurrung and J. Fajans, Phys. Fluids B **2**, 693 (1990).
[8] A.J. Peurrung and J. Fajans, Phys. Fluids B **5**, 4295 (1993).
[9] Y. Kiwamoto, K. Ito, A. Sanpei, A. Mohri, T. Yuyama and T. Michishita, J. Phys. Soc. Jpn. **68**, 3766 (1999).
[10] K. Ito, Y. Kiwamoto and A. Sanpei, Jpn. J. Appl. Phys. Part 1 **40**, 2558 (2001).
[11] D.L. Eggleston, C.F. Driscoll, B.R. Beck, A.W. Hyatt and J.H. Malmberg, Phys. Fluids B **4**, 3432 (1992).